Analytical-FE modeling of high-speed dry machining of the aeronautical aluminium alloy AA2024–T351

Y. Avevor[1], A. Moufki[1], M. Nouari[2]

[1]Laboratoire d'Etude des Microstructures et de Mécanique des matériaux, LEM3, UMR-CNRS 7239, Université de Lorraine, Ile de Saulcy ,57045, Metz, France

[2]Laboratoire d'Energétique et de Mécanique Théorique et Appliquée, LEMTA CNRS-UMR 7563, Mines Nancy, Mines Albi, GIP-INSIC,27 rue d'Hellieule ,88100 Saint-Dié-des-Vosges, France

Abstract

In dry high speed machining of aluminium alloy AA2024-T351, the thermomechanical process of chip formation, the tool wear and the surface integrity depend strongly on the tribological conditions along the tool rake face. In the present work, we propose a hybrid Analytical-FE model taking into account the thermomechanical coupling between the chip formation process and the sticking-sliding conditions at the tool-chip interface. The transient nonlinear thermal problem in the tool-chip-workpiece system is solved by using a Petrov-Galerkin finite element model. The model has been compared to the experimental data for a wide range of cutting speeds. This comparison shows a good agreement in both trends and values for cutting forces and tool-chip contact length. It has been also observed that a transition from a sliding contact to a sticking–sliding contact occurs when the local friction coefficient and the thermal softening are large enough.

Keywords:
Primary shear zone, Secondary shear zone, sliding/sticking contact, local friction coefficient, apparent friction coefficient, frictional heat partition.

1 INTRODUCTION

In dry high speed machining of aluminium alloy AA2024-T351, the friction conditions at the tool-chip interface and along the round cutting edge are very complex. Several studies have shown that the tool wear is mainly caused by the built-up layer (BUL) formation along the tool rake face, [1-5]. The BUL is an adhesive interaction between the work material and the tool rake face. It forms when the local friction coefficient, in the sliding zone, and the temperature at the tool-chip interface are large enough, [6-8].

It should be noted that to understand the friction effects in machining, we have to analyse the inherent relationship among, the cutting conditions (cutting and feed velocities, tool geometry), the workpiece material behaviour, the thermomechanical characteristics of the tool material, the frictional heat partition in the sliding zone and the friction conditions at the tool-chip and tool-workpiece interfaces. Due to the problem complexity, it appears that despite many works on machining of Aluminium alloy, the understanding of the effect of friction conditions requires further investigations.

To predict correctly the influences of contact conditions, we have to develop an appropriate model of chip formation taking into account the interaction between the process formation of sticking zone along the tool rake face (tribological conditions) and the thermomechanical material flow in the primary shear zone.

Several authors have proposed different simplified approaches to model the effects of cutting conditions on the sticking-sliding zones at the tool-chip interface. For instance, the contact has been assimilated to a pure sliding contact in [9] and to a pure sticking contact in [10]. The finite element method was also often used to analyze the friction effects, [8, 11-16]. According to the literature works, it appears that due to the complexity of the tool–chip contact, the tribological conditions are not fully understood and accurate predictive models have yet to be developed, [11-16].

In the present work, to identify the interaction between the thermomechanical phenomena at the tool-chip interface and the material flow in the primary shear zone; an analytical model has been coupled with a finite element approach. The transient nonlinear thermal problem in the tool-chip-workpiece system has been solved by using a FE model based on the Petrov-Galerkin formulation. The coupling between the primary shear zone (PSZ) (chip formation), the secondary shear zone (SSZ) (sticking zone) and the frictional heat at the sliding zone has been taking into account. The model allows to determine in a fast and simple way several significant machining parameters as: (i) the cutting forces, (ii) the temperature distribution in the tool-chip-workpiece system, (iii) the heat flux from the PSZ to the workpiece, (iv) the tool-chip contact length, (v) the frictional heat partition coefficient and (vi) the local friction coefficient in the sliding zone.

2 CHIP FORMATION PROCESS: AN ANALYTICAL-FE MODEL

In machining, the thermal problem is a nonlinear heat and mass transfer problem involving the combined effects of transport and diffusion. The temperature distribution $T(x,y)$ is governed by the heat equation:

$$k\left(\frac{\partial^2 T}{\partial x^2}+\frac{\partial^2 T}{\partial y^2}\right)+Q=\rho c\frac{DT}{Dt} \quad (1)$$

with

$$\begin{cases} Q = Q_{PSZ}(x,y) + Q_{SSZ}(x,y) + Q_f(\tilde{x})\delta(\tilde{y}) \\ \dfrac{DT}{Dt} = \dfrac{\partial T}{\partial t} + \mathrm{v}(x,y)\dfrac{\partial T}{\partial x} + \mathrm{u}(x,y)\dfrac{\partial T}{\partial y} \end{cases} \quad (2)$$

where Q_{PSZ} and Q_{SSZ} designate respectively the heat source due to the viscoplastic deformation in the primary and secondary shear zones. Q_f is the heat source due to the frictional contact in the sliding zone:

$$Q_{SSZ} = \tau_{st} V_c / h_2, \quad Q_f = \mu_{sl} V_c \, p_0 (1 - \tilde{x}/l_c)^{\xi} \quad (3)$$

with V_c, h_2, p_0, l_c and μ_{sl} represent respectively the bulk chip velocity, the width of the secondary shear zone, the pressure exerted on the tool tip, the tool-chip contact length and the local friction coefficient at the tool-chip interface, see Fig. 1. The coordinates $(\tilde{x}, \tilde{y})$, reported in Fig. 1, are associated to the tool rake face where the pressure distribution is characterized by ξ.

In Eq. (2), the parameters ρ, c, k, $\mathrm{u}(x,y)$ and $\mathrm{v}(x,y)$ represent respectively the material density, the heat capacity, the thermal conductivity and the components of material velocity in x and y directions.

Note that the introduction of Dirac function $\delta(\tilde{y})$ allows to take into account easily the partition of the frictional heat source $Q_f(\tilde{x})$ between the tool and the chip. In the secondary shear zone, the effect of the strain hardening is supposed to be neglected with respect to strain rate and thermal effects. Thus, the shear stress τ_{st} in this zone is determined from the Johnson–Cook law (5) by considering: $\gamma = \gamma_h$ (which is the shear strain at the exit of the primary shear zone given by Eq. (5.2)) and $\dot{\gamma} = V_c / h_2$.

The thermoviscoplastic behaviour of the workpiece material is assumed to be isotropic and given by the Johnson–Cook law:

$$\tau = \frac{1}{\sqrt{3}}\left[A + B\left(\frac{\gamma}{\sqrt{3}}\right)^n\right]\left[1 + C\ln\left(\frac{\dot{\gamma}}{\dot{\gamma}_0}\right)\right]\left[1 - \left(\frac{T - T_0}{T_m - T_0}\right)^m\right] \quad (4)$$

where τ, $\dot{\gamma}$, γ and T represent respectively the shear stress, the shear strain rate, the shear strain and the temperature. The characteristics of the work material behaviour are the strain hardening exponent n, the strain rate sensitivity coefficient C, the thermal softening exponent m and the constants A, B, $\dot{\gamma}_0$, T_0 (reference temperature) and T_m (melting temperature).

The primary shear zone (PSZ) is assumed to be a thin band of constant thickness h_1 and it is characterized by the shear angle ϕ, see Fig. 1. This assumption is reasonable when the cutting speed is large enough as in high speed machining. In addition, this zone is decomposed into a set of elements with thickness h_1 and width dl as shown in Fig. 1. To model the material flow within each element '*i*', the stationary one-dimensional approach developed in [25-27] has been modified to take into account the coupling between the material flow in the PSZ and the nonlinear thermal problem. Thus, in the present work we suppose a quasi-stationary flow in each element '*i*' where the shear velocity v_s, the shear strain γ, the shear strain rate $\dot{\gamma}$ and the shear stress τ depend only on the coordinate y_s along the normal to this band and on the mean temperature $\bar{T}_i$ in the element '*i*'. By using the one-dimensional formulation, we get:

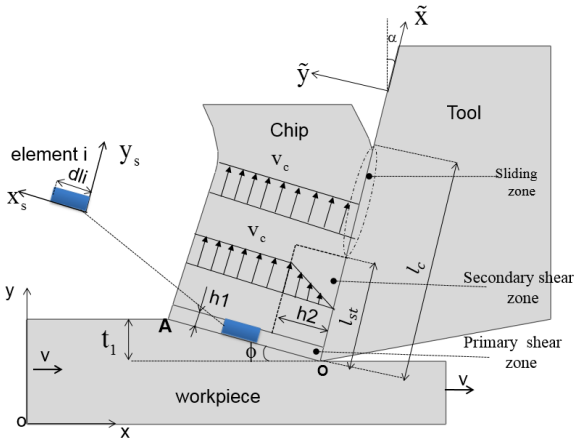

Figure 1: Illustration of an orthogonal cutting operation

$$\begin{cases} \tau = \tau(v_s, \tau_0) = \rho\, V \sin(\phi)\, v_s + \tau_0, \\ \gamma = v_s / V \sin\phi \\ \dot{\gamma} = \psi(v_s, \tau_0), \quad dv_s / dy_s = \psi(v_s, \tau_0) \end{cases} \quad (5)$$

where the function ψ is deduced from the JC law (1) by considering the mean temperature $\bar{T}_i$ in the element '*i*'.

From the boundary conditions corresponding the PSZ : $v_s(y_s = 0) = 0$, $v_s(y_s = h_1) = V\cos\alpha / \cos(\phi - \alpha)$, the integration of the nonlinear differential equation (5.4) leads to an integral equation which is solved numerically to determine the shear stress τ_0 at the entry of the primary shear zone for each element '*i*'. In addition, by considering the average value $\bar{q}_i$ of the viscoplastic heat source $\beta\tau\dot{\gamma}$ in '*i*', the heat source Q_{PSZ} can be estimated as following.

$$Q_{PSZ} = \sum_i \bar{q}_i \quad with \ \bar{q}_i = \frac{\beta}{h_1}\int_0^{h_1} \tau\dot{\gamma}\, dy_s \quad (6)$$

β is the Taylor-Quinney coefficient (the fraction of plastic work converted into heat).

According to [27, 2-4], p_0 and l_c are obtained from the chip equilibrium which leads to:

$$p_0 = 4\frac{(1+\xi)}{(2+\xi)}\frac{\cos^2\bar{\lambda}}{\sin\left(2\left(\phi + \bar{\lambda} - \alpha\right)\right)}\frac{F_s}{w\, l_{OA}}$$
$$l_c = t_1\frac{(2+\xi)}{2}\frac{\sin\left(\phi + \bar{\lambda} - \alpha\right)}{\sin(\phi)\cos(\bar{\lambda})} \quad (7)$$

with $\bar{\lambda} = tan^{-1}(\bar{\mu})$ and w represent respectively the apparent friction angle at the tool-chip interface and the width of cut. At the at the exit of the primary shear zone, the shearing force F_s is given by :

$$F_s = \int_0^{l_{OA}} \tau(y_s = h_1)\, w\, dx_s \quad (8)$$

where the length $l_{OA} = t_1 / \sin\phi$ is defined in Fig. 1.

At the tool-chip interface, the equations governing the sticking zone length l_{st} (in Fig1, the length *a* of the sticking zone has to be substituted by l_{st}) and the relationship between the local friction coefficient μ_{sl} in the sliding zone and the apparent fiction coefficient $\bar{\mu}$ are respectively obtained from the shear stress continuity at the tool-chip interface and from the chip equilibrium, see [10,11]:

$$\mu_{sl}\frac{p_0}{\tau_{st}(x=l_{st})}\left(1-\frac{l_{st}}{l_c}\right)^{\xi}-1=0$$

$$\mu_{sl}\left(1-\frac{l_{st}}{l_c}\right)^{\xi}\left(\frac{(1+\xi)}{\tau_{st}(x=l_{st})l_c}+\%_{st}+1-\frac{l_{st}}{l_c}\right)-\bar{\mu}=0 \qquad (9)$$

$$\%_{st}=\int_0^{l_{st}}\tau_{st}(x)\,dx$$

In the implicit equations (9) the shear stress $\tau_{st}(x)$ at the tool chip interface (i.e. $y=0$) for $0\le x\le l_{st}$ (sticking zone) is calculated from (4) as indicated previously. To determine the temperature $T(x,y)$ in the tool-chip-workpiece system, the nonlinear heat mass transfer is solved by using the FE method based on the Petrov-Galerkin approach. The implicit Euler scheme which is unconditionally stable in time has also been combined with the Newton-Raphson method to solve the thermal nonlinear problem at each time *t*.

3 RESULTS AND DISCUSSIONS

To validate the present model, the predicted results was compared with the experimental measurements reported in [12] for orthogonal cutting tests of aluminum alloy AA2024–T351 under dry cutting conditions by using an uncoated carbide insert. The cutting speed *V* was chosen in the range from 80 to 500 m/min. The rake angle α is equal to 0°. The uncut chip thickness t_1 and the width of cut w were respectively fixed to 0.1 mm. and 4 mm.
According to [8], the work material and tool parameters are summarized in Table1 and (10).

Table1 Thermomechanical parameters.

Parameters	Workpiece	Tool
Density, ρ [kg.m^{-3}]	2780	15000
Thermal conductivity, k [W.m^{-1}.K^{-1}]	120	100
Specific heat, c_p [J.kg^{-1}.K^{-1}]	856	240

For the aluminum alloy AA2024–T351, the Johnson–Cook law parameters are given by:

$$\begin{cases} A=265\,MPa \quad B=426\,MPa \\ n=0.34 \quad C=0.015 \quad m=1 \\ T_m=775\,K \quad T_0=293\,K \end{cases} \qquad (10)$$

The measured cutting forces and contact length are reported in Figs. 2 and 3. From these trends, it appears that the cutting forces and the tool–chip contact length l_c are decreasing functions of V. This decay is due the thermal softening of the work material along the tool rake face. Indeed, one of the relevant parameters for chip formation process during its interaction with the cutting tool is the temperature at the tool –chip interface. In fact, this temperature controls the thermal softening of the work-material and affects the whole process. The predicted temperature along the tool rake face is shown in Fig. 5 where the temperature increases with the cutting speed. This tendency is caused by (a) the self-heating of the work material due to plastic deformation in the primary and secondary shear zones, (b) the frictional heating along the sliding zone. Thus, when this thermal softening and the local friction coefficient μ_{sl} are large enough, the interface shear stress τ_{st} becomes smaller and the tool-chip contact is governed by sticking conditions (i.e. $\mu_{sl}\,p>\tau_{st}$ with *p* is the contact pressure). The Fig. 6 shows this fact through the growing of the sticking zone length l_{st} and the ratio l_{st}/l_c in terms of V.

Consequently, the forgoing tendencies reveal that the variation of the cutting forces and the apparent friction coefficient $\bar{\mu}$ (see Fig. 4) in terms of cutting velocity is mainly controlled by the decay of the interface shear stress τ_{st} caused by the thermal softening. In addition, the evolution of l_c is also related to this fact through $\bar{\mu}$.

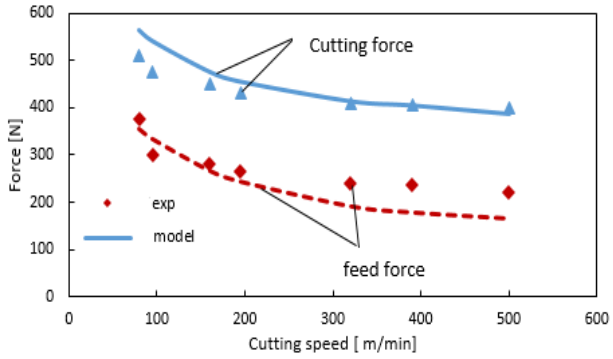

Figure 2: Comparison between the model results and the experimental cutting forces for different cutting speeds.

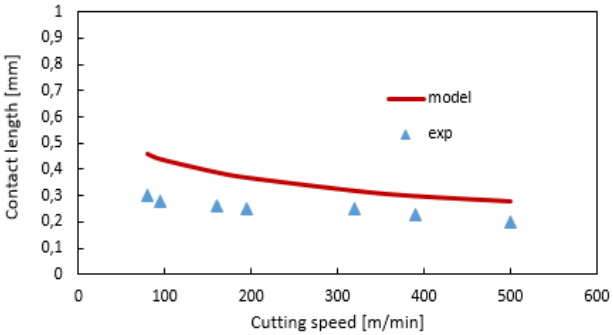

Figure 3: Effect of the cutting speed the tool-chip contact length.

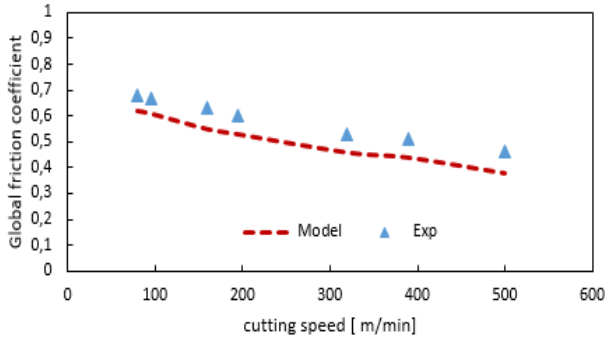

Figure 4: Variation of the apparent friction coefficient in function of cutting velocity.

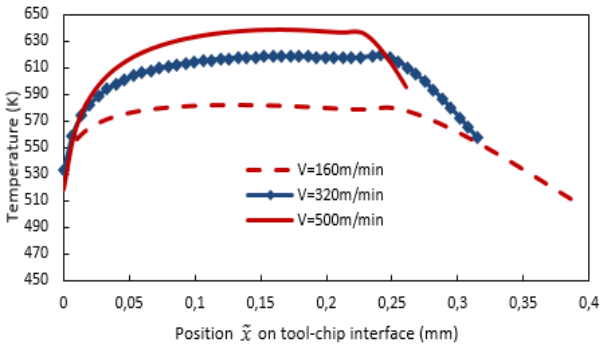

Figure 5: Influence of the cutting speed on the temperature distribution at the tool-chip interface.

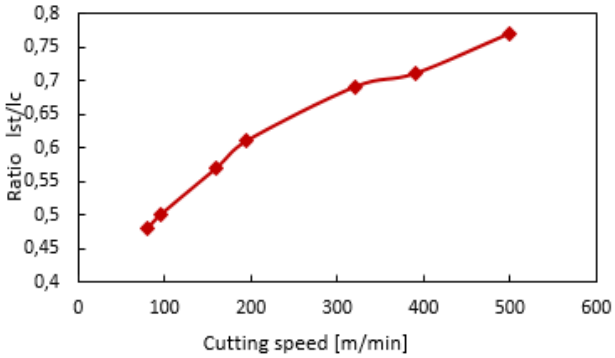

Figure 6: Variation of the ratio l_{st}/l_c , predicted by the model, in function of cutting the temperature distribution evolution at tool-chip.

4 CONCLUSION

To analyse the inherent relationship among the work material behaviour, the thermomechanical characteristics of the tool material, the cutting conditions (cutting and feed velocities, tool geometry) and the friction conditions at the tool-chip interface, a hybrid Analytical-FE model has been proposed in the present work. The analytical approach has been used to model the material flow in the primary shear zone, the tool–chip contact length, the link between the local friction coefficient, the sliding–sticking zones and the apparent friction coefficient which can be estimated from cutting forces measurements. In addition, the transient FE model takes into account the coupling between the primary shear zone (chip formation), the secondary shear zone (sticking zone) and the frictional heat at the sliding zone. The model allows to determine in a fast and simple way several significant machining parameters. The comparison between experiment and model shows a good agreement in both trends and values for cutting forces and tool-chip contact length.

5 REFERENCE

1. M. Nouari, G. List, F. Girot, D. Géhin. “Effect of machining parameters and coating on wear mechanisms in dry drilling of aluminium alloys.” *International Journal of Machine Tools & Manufacture* 45 (2005) 1436–42.
2. Nouari M, List G, Girot F, Coupard D, “Experimental analysis and optimization of tool wear in dry machining of aluminium alloys”. *Wear 255;* 2003, p.1359 1368.
3. P.Eh. Hovsepian, Q. Luo, G. Robinson, M. Pittman, M. Howarth, D. Doerwald, R. Tietema, W.M. Sim, A. Deeming, T. Zeus. “TiAlN/VN superlattice structured PVD coatings: a new alternative in machining of aluminium alloys for aerospace and automotive components”. *Surface and Coatings Technology*, 201 (2006), 265–272.
4. G. List, M. Nouari, D. Géhin, S. Gomez, J.P. Manaud, Y. Le Petitcorps, F. Girot, “Wear behaviour of cemented carbide tools in dry machining of aluminium alloy”, *Wear 259* (2005) 1177–1189
5. M.S. Carrilero, J.M.S. Sola, J.M. Sanchez, M. Alvarez, A. Gonzalez, J.M. Marcos, “A SEM and EDS insight into the BUL and BUE differences in the turning process of AA2024 Al–Cu Alloy”, *Int. J. Mach. Tools Manuf.* 42 (2002) 215–220.
6. S. Bahi, M. Nouari, A. Moufki, M. El Mansori, A. Molinari. “A new friction law for sticking and sliding contacts in machining.” *Tribology International,* 44 (7–8), 2011, 764-771.
7. S. Bahi, M. Nouari, A. Moufki, M. El Mansori, A. Molinari. “Hybrid modelling of sliding–sticking zones at the tool–chip interface under dry machining and tool wear analysis.” *Wear, 286–287*, 2012, 45-54.
8. S. Atlati, B. Haddag, M. Nouari, A. Moufki.” Effect of the local friction and contact nature on the Built-Up Edge formation process in machining ductile metals”. *Tribology International,* 90, 2015, 217-227.
9. E. Merchant. “Mechanics of the metal cutting process. II. Plasticity conditions in orthogonal cutting.” *J. Appl. Phys.,* 16 (1945), pp. 318–324.
10. P.L.B. Oxley. “Mechanics of Machining”. *Ellis Horwood, Chichester*, UK (1989).
11. T.H.C. Childs, K. Maekawa, T. Obikawa, Y. Yamane. “Metal Machining: Theory and Applications.” Copublished in North, Central and South America by John Wiley & Sons Inc., New York/Toronto (2000) pp. 65–68.
12. T. Ozel. “The influence of friction models on finite element simulations of machining”. *Int. J. Machine Tools Manuf.*, 46 (2006), pp. 518–530.
13. L. Filice, F. Micari, S. Rizzuti, D. Umbrello. “A critical analysis on the friction modelling in orthogonal machining”. *Int. J. Machine Tools Manuf.*, 47 (2007), pp. 709–714.
14. A.J. Haglund, H.A. Kishawy, R.J. Rogers. “An exploration of friction models for the chip-tool interface using an Arbitrary Lagrangian–Eulerian finite element model”. *Wear, 265* (2008), pp. 452–460
15. P.J. Arrazola, T. Özel. “Investigations on the effects of friction modeling in finite element simulation of machining”. *Int. J. Mech. Sci.,* 52 (1) (2010), pp. 31–42.
16. T.H.C. Childs. “Friction modelling in metal cutting.” *Wear,* 260 (2006), pp. 310–318.